INL/EXT-15-36752

Light Water Reactor Sustainability Program

Fracture Capabilities in Grizzly with the eXtended Finite Element Method (X-FEM)

September 2015

DOE Office of Nuclear Energy

DISCLAIMER

This information was prepared as an account of work sponsored by an agency of the U.S. Government. Neither the U.S. Government nor any agency thereof, nor any of their employees, makes any warranty, expressed or implied, or assumes any legal liability or responsibility for the accuracy, completeness, or usefulness, of any information, apparatus, product, or process disclosed, or represents that its use would not infringe privately owned rights. References herein to any specific commercial product, process, or service by trade name, trade mark, manufacturer, or otherwise, do not necessarily constitute or imply its endorsement, recommendation, or favoring by the U.S. Government or any agency thereof. The views and opinions of authors expressed herein do not necessarily state or reflect those of the U.S. Government or any agency thereof.

INL/EXT-15-36752

Light Water Reactor Sustainability Program

Fracture Capabilities in Grizzly with the eXtended Finite Element Method (X-FEM)

John Dolbow[1], Ziyu Zhang[1], Benjamin Spencer[2], Wen Jiang[2]

[1]Duke University
[2]Idaho National Laboratory

September 2015

Idaho National Laboratory
Idaho Falls, Idaho 83415

http://www.inl.gov/lwrs

Prepared for the
U.S. Department of Energy
Office of Nuclear Energy
Under DOE Idaho Operations Office
Contract DE-AC07-05ID14517

EXECUTIVE SUMMARY

Efforts are underway to develop fracture mechanics capabilities in the Grizzly code to enable it to be used to perform deterministic fracture assessments of degraded reactor pressure vessels (RPVs). A capability was previously developed to calculate three-dimensional interaction integrals to extract mixed-mode stress-intensity factors. This capability requires the use of a finite element mesh that conforms to the crack geometry.

The eXtended Finite Element Method (X-FEM) provides a means to represent a crack geometry without explicitly fitting the finite element mesh to it. This is effected by enhancing the element kinematics to represent jump discontinuities at arbitrary locations inside of the element, as well as by incorporating asymptotic near-tip fields to better capture crack singularities. In this work, use of only the discontinuous enrichment functions was examined to see how accurate stress intensity factors could still be calculated.

This report documents the following work to enhance Grizzly's engineering fracture capabilities by introducing arbitrary jump discontinuities for prescribed crack geometries:

- X-FEM Mesh Cutting in 3D: to enhance the kinematics of elements that are intersected by arbitrary crack geometries, a mesh cutting algorithm was modified to permit the definition of arbitrary elliptical cracks in 3D solids.
- Interaction Integral Modifications: the existing code for evaluating the interaction integral in Grizzly was based on the assumption of a mesh that was fitted to the crack geometry. Modifications were made to allow for the possibility of a crack front that passes arbitrarily through the mesh.
- Benchmarking for 3D Fracture: the new capabilities were benchmarked against mixed-mode three-dimensional fracture problems with known analytical solutions.

CONTENTS

FIGURES

ACRONYMS

LEFM	Linear Elastic Fracture Mechanics
LDRD	Laboratory-Directed Research and Development
LWRS	Light Water Reactor Sustainability
PWR	Pressurized Water Reactor
XFEM	eXtended Finite Element Method
SIF	Stress Intensity Factor

1 Introduction

The Grizzly code is being developed to address aging issues in a variety of nuclear power plant systems, structures, and components under funding from the Department of Energy's Light Water Reactor Sustainability (LWRS) program. The initial application of Grizzly is to study the effects of aging in reactor pressure vessels (RPVs). RPVs that have been subjected to long-term exposure to irradiation and elevated temperatures experience embrittlement of the steel, which increases the susceptibility to fracture. To assess that, it is necessary to have both engineering fracture mechanics capabilities (to assess stress intensities at pre-existing flaws) and capabilities to model the material embrittlement process.

Development in prior years has provided Grizzly with the capability to perform deterministic fracture assessments of RPVs. This capability was based on performing fracture integrals for three-dimensional cracks that were explicitly fitted with a finite element mesh. Creating such meshes, especially in three dimensions, is a labor-intensive process. This makes it challenging to consider a distribution of crack sizes, for example, to better obtain insight into the probability of failure. For the RPV fracture problem, evaluating surface-breaking flaws that slightly penetrate through the cladding into the base material is of particular interest, and generating meshes fitted to the flaw is especially challenging in that case. Moreover, simulating crack growth with meshed cracks would require algorithms for three-dimensional remeshing. While such algorithms have improved considerably over the past several decades, they are nonetheless limited to single cracks.

The eXtended Finite Element Method (X-FEM) was introduced in [2] as a means to circumvent these fundamental issues. The X-FEM allows for cracks to be "embedded" with respect to an underlying finite element mesh. By embedded here, we mean that the mesh need not explicitly fit the crack geometry. The X-FEM accomplishes this by enriching the finite-element approximation in two basic ways. First, it provides a type of generalized Heaviside enrichment which allows for the crack faces to separate along an arbitrary surface inside of the element. Second, it enriches with near-tip asymptotic functions to capture the singular fields near crack fronts.

An implementation of the X-FEM in the MOOSE framework upon which Grizzly is based has been under development under another funding from a Laboratory-Directed Research and Development (LDRD) project at Idaho National Laboratory over the past three years. In the past year, funding from the LWRS program was used to build on that work to enable the computation of stress intensity factors (SIFs) on arbitrary flaws in three-dimensional solids, to permit its used for assessing fracture in RPVs.

The implementation of the X-FEM in MOOSE is based on the phantom node method of [3], which was shown in [4] to be equivalent to the original X-FEM formulation with Heaviside enrichment. In the original X-FEM formulation, additional degrees of freedom are introduced at all nodes connected to finite elements that are traversed by crack paths to account for the discontinuity. This can present some implementational issues in an existing finite element code because significant changes need to be made to permit arbitrary numbers of degrees of freedom in each element, and this can be particulary challenging in elements where cracks branch or merge, where even more degrees of freedom need to be added.

In the phantom node method, the discontinuity in the solution fields is introduced by splitting the finite element mesh everywhere that it is traversed by a crack. Elements that are split by a crack are removed and replaced by two overlapping "partial" elements that are properly connected to reflect the topology of the crack. These partial elements each represent a part of the physical domain of the original element that they replaced, and together, they represent the entire original domain. The solution fields are interpolated across the entire domain of the partial elements, but when quantities are integrated over the elements, the integral is only performed over the physical part. A significant benefit of the phantom node method is that it naturally permits the representation of crack branching by recursively subdividing partial elements.

To enable the phantom node in a finite element code requires an algorithm that cuts and reconnects the mesh appropriately to represent the effect of the discontinuity introduced by cracking, and modifications to the integration algorithms to permit integration of quantities over partial elements.

Using only Heaviside enrichment with the X-FEM introduces two issues related to accuracy in terms of calculating SIFs. First, the lack of near-tip enrichment means that the singular nature of the fields have to be captured using only the classical piecewise-linear polynomial functions. The second aspect concerns effective changes to the crack front geometry that are introduced. Near-tip enrichment allows the precise geometry of the crack front to be represented. Without it, and using only Heaviside enrichment, cracks must terminate along element faces. This introduces a somewhat artificial change to the crack geometry, albeit one that vanishes with increasing refinement. So while reasonably accurate SIFs might still be attainable with mesh refinement, this approach limits the accuracy that can be obtained on coarse meshes.

The work documented here, which was performed to enable the use of the X-FEM for the Grizzly application consisted of the following:

- Modification of the previously-developed mesh cutting algorithm to permit the definition of arbitrary circular and elliptical cracks in 3D models.
- Modifying the code for fracture domain integrals to permit its use with cracks represented with the X-FEM.
- Testing of the fracture domain integrals with the X-FEM on a series of benchmark problems in three-dimensional fracture mechanics to verify that the results match known analytical solutions.

This report is organized according to the tasks taken in this project. Section 2 describes the implementation of the element fragment algorithm and the modifications to the interaction integral routines. Section 3 documents the benchmarking of the new capabilities against problems with analytical solutions and one in RPV fracture. Finally, Section 4 provides a summary of this work.

2 Implementation Details

As mentioned previously, the X-FEM implementation in MOOSE/Grizzly is based on the phantom node method of [3]. The major components required to implement this technique include a mesh cutting algorithm and modification the integration routines to handle partial elements. To permit the use of the X-FEM to compute SIFs along crack fronts in 3D models, which is of interest for the Grizzly application, the interaction integral routines were modified to permit the evaluation of those integrals along a pre-specified array of points corresponding to the embedded crack front. Implementation details of the mesh cutting algorithm and interaction integral routines are provided here.

2.1 Mesh Cutting Algorithm

The mesh cutting algorithm that has been implemented in Grizzly is based on the approach described in [1]. Consider a small collection of elements that are intersected by two cracks as shown on the left in Figure 1. When a crack geometry is arbitrarily superimposed over a mesh in this way, the standard finite elements cannot represent all of the requisite kinematics across the crack surfaces. This includes, primarily, the jump in the displacement field that is expected across a crack interior.

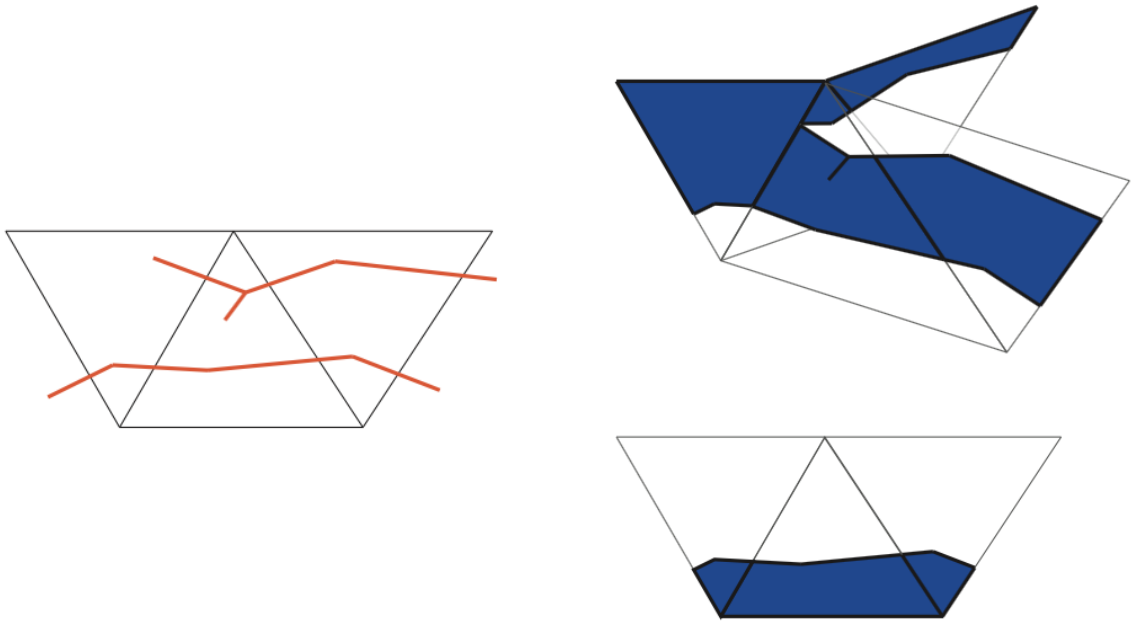

Figure 1: A set of elements intersected by an arbitrary crack network (left) and a collection of partial elements with the proper kinematics, representing a cut mesh (right). Figured adopted from [1].

The mesh cutting algorithm addresses this by replacing the elements that are intersected by the crack geometry with a new set of partial elements and virtual nodes, as shown on the right of Figure 1. The virtual nodes correspond to standard shape functions, they just happen to be located outside of the physical domain. In practice, the application of this algorithm results in enhanced kinematics that are very close to what can be obtained using Heaviside enrichment with the standard X-FEM.

We now describe the steps in the algorithm. At the beginning of each time step, the element fragment algorithm breaks down to seven steps, as introduced below.

2.1.1 Update element neighbors

For each face of each element, the neighboring elements, if any, are stored. These neighbor relationships are used later on to check to see whether the partial elements potentially created as children of these elements share material connections. They are also used to identify elements that are at a crack tip as of the last pass through the cutting algorithm.

From the perspective of the current element for which neighbors are being established, the criterion for considering another element to be a neighbor connected to a given face is that the neighbor has a face with the same nodes as the current element face, and that the other element doesn't overlay the current element. In the actual implementation, the information about neighbors is stored in each element according to its sides. The procedure for this step is essentially the same for 2D and 3D.

2.1.2 Mark elements at crack tip

To allow for dynamic propagation of a crack through the mesh, partial elements at the crack tip must receive special treatment. In general, a crack tip is represented by merging the nodes of two partial elements on a common side where the crack terminates. In Figure 2 for instance, Element 5 and 6 are merged together on the edge connected by Node 2 and 5 (Edge 2-5), and they are called crack-tip-split elements in our terminology. The crack terminates on the left edge of Element 2, but does not split that element, which is called a crack-tip element. A crack-tip element contains a single fragment, and the boundary of that fragment at the crack tip has been split into two segments.

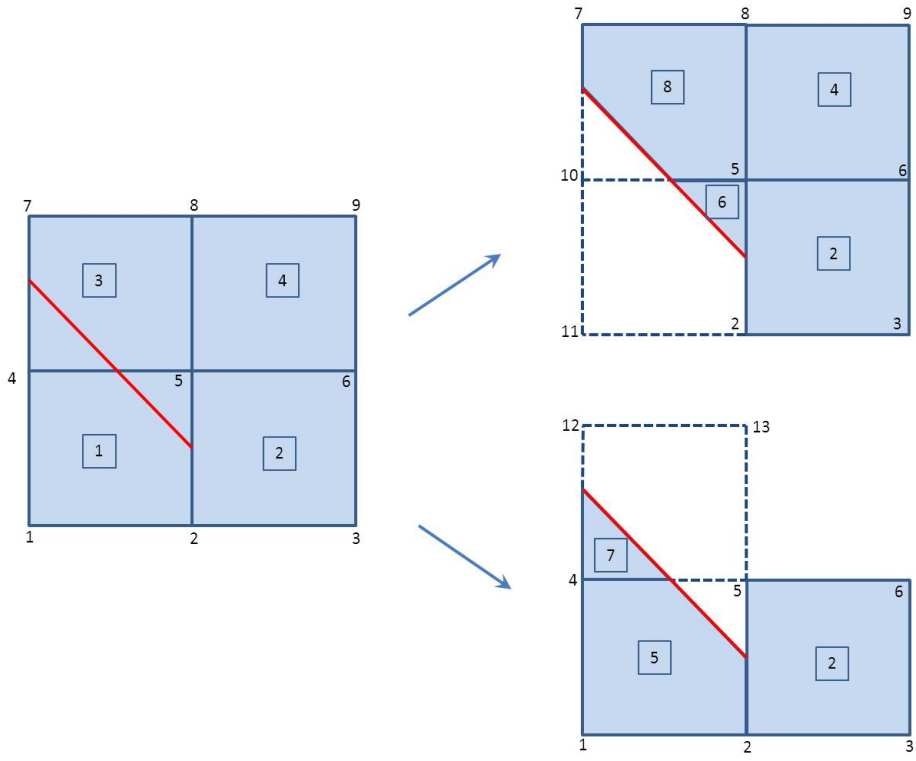

Figure 2: A crack tip element and its neighboring partial elements in two dimensions. The left figure is the mesh before mesh cutting and the right two figures show the partial elements on each side of the crack, respectively. The boxed numbers are element IDs and the shaded areas are the physical domains of partial elements. The red line represents the crack position.

In three dimensions, the definition of crack-tip-split elements is more complicated. Figure 3 illustrates a three-dimensional crack tip scenario from the top view, where Elements 2, 3 and 4 will be fully split and Element 1 will be a crack-tip element since it only has two sides being cut but the element itself is not split. The two children of Elements 2 or 3 can be easily identified as crack-tip-split elements since both of them will share a common face with Element 1. However, this is not true for the two children of Element 4 because they only share a common edge with Element 1 while the neighbor information of each element is stored according to its faces. The solution of this problem will be introduced in Section 2.1.5.

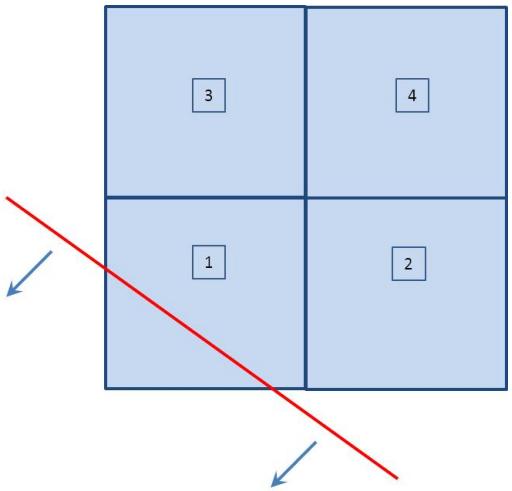

Figure 3: Top view of a crack tip element and its neighboring elements in three dimensions before they are split. The red line represents a crack front and the blue arrows indicate the direction of crack extension. We note that the two children of Element 4 are not identified as a crack-tip-split element.

2.1.3 Mark new cuts

Elements to be cut can be marked based on geometric criteria or physical behavior of the material. In three dimensions, we find the intersection between element faces and the cut plane by first computing the intersection on the face edges. An element face is regarded as being split only if two edges of that face intersect with the cut plane. Thus, the faces with only one edge intersected by the cut plane will be automatically ignored in the marking process.

2.1.4 Create fragments

A central aspect of the element fragment algorithm is the definition of the physical part of each element using fragment data structures, which define the boundary of the physical portion of a given element using a combination of embedded nodes and standard finite element nodes (also called permanent nodes in our terminology). A three-dimensional fragment is defined by its boundary faces (see Figure 4).

Previously uncut elements or fragments that are to be split by a cut plane in the current step are split into a set of new fragments that combine together to cover the entire element or old fragment. Elements or fragments that are not split by a cut plane, but have sides that are intersected by cut planes include the embedded nodes on those sides. These elements/fragments end up producing new special fragments that have collinear sides contained by the corresponding host element side. Per the definition in Section 2.1.2, such elements are the crack-tip elements. Elements that are not touched by any cut planes, and thus contain no embedded nodes, contain no fragments.

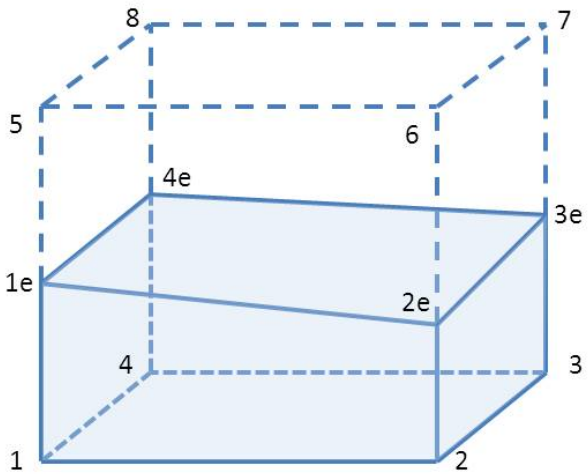

Figure 4: A fragment owned by a hex element in three dimensions. The fragment is defined by six faces: Face 1-4-3-2, Face 1-2-2e-1e, Face 2-3-3e-2e, Face 3-4-4e-3, Face 4-1-1e-4e and Face 1e-2e-3e-4e. The suffix “e" indicates an embedded node produced by the intersection between the cut plane and element face edges.

We note that special care must be taken for crack-tip elements before new fragments are actually created. Considering that each of these elements already owns a fragment with collinear boundary sides, and that the common set of the two collinear sides (which is an embedded node in two dimensions and an edge in three dimensions) implicitly indicates an intersection, we must re-combine the two collinear sides to form a single intersected side for the algorithm not to miss one intersection when it tries to count the total intersections.

2.1.5 Create child elements from fragments

Each element that contains more than one fragment will be split into multiple elements, one for each fragment in that element. A child element is created for each fragment. The same node numbering used for the parent element is used for each child element, except that the nodes that are not contained in the fragments are replaced with temporary nodes. Before the step of creating child elements, an element may already have a single fragment because it has been cut previously and is not being cut by a secondary crack in the current step. In such a situation, this element does not create child elements. The elements with no fragment do not create children either because they are not touched by any cutting planes, and do not require special treatment.

We note that if a non-crack-tip-split element has a phantom node connected to a crack tip side that will be split, this element must create a child for itself to avoid the non-physical scenario where two partial elements are connected at a phantom node. This special treatment also takes care of the issue of three-dimensional “edge neighbors" not being marked as crack-tip-split elements as mentioned in Section 2.1.2.

2.1.6 Connect neighboring fragment child elements

A loop is made through every parent element in the mesh. For each parent element, every child element is matched with every child element of the neighboring parent elements. If the neighboring child elements share a material connection, the nodes on the common face are merged. From the perspective of any child element, this is done by looping over all the children of its parent’s neighbors and properly collapsing relevant DOFs. This algorithm is also applicable to three dimensions.

2.1.7 Clear old ancestry

All information about parent/child relationships between elements and nodes is cleared. The result of this is that in subsequent time steps, neighbor relationships are based on the connections between the partial elements rather than between the parent elements that they were created from. This removes all connection between the material on opposing sides of the interface, and permits partial elements to be split multiple times, as would occur with crack branching.

2.2 Interaction Integral Modifications

The interaction integral is essentially a means to extract mixed-mode stress intensity factors (SIFs) from a computation of a problem in fracture mechanics. With the finite element method, it is normally calculated in a post-processing step as a domain integral over a finite sized volume in the vicinity of a point on the crack front. The integrand involves a combination of numerical and “auxiliary" fields, the former being the finite element approximation and the latter being known asymptotic solutions for fracture problems. By constructing the auxiliary fields to correspond to pure Mode-I, Mode-II, and Mode-III load cases, the contribution of the actual field as approximated by the finite element method to each SIF can be ascertained.

In the standard finite element method, the finite element mesh is built to match the crack front geometry. Normally the mesh is also constructed such that groups of elements for use in the domain integrals that comprise the interaction integral can be easily determined and used. With X-FEM enrichment, the mesh is not designed to match the crack geometry, and as such, no such domains exist.

As a result, Grizzly was modified in this work to allow the interaction integral to be calculated using only a set of points along the crack front as specified by the user. The width of the interaction integral domain, as it relates to the weight function q, is also provided as an input. These changes were relatively straightforward to introduce, and they only require knowledge of the crack geometry. The crack front is now described by a pre-specified array of points corresponding to the embedded front. Currently, both straight crack fronts and curved crack fronts, such as circular and elliptical-shaped cracks, are supported. With the pre-specified crack front points, the subroutine that generates the q function based on the distance of a point from the crack front was implemented. For the domain integral, several integration methods for the cut element are provided, such as volume fraction and moment-fitting methods.

3 Benchmarking for Three-Dimensional Fracture

We now look at a sequence of standard three-dimensional benchmark problems in linear elastic fracture mechanics (LEFM). In particular we consider problems with planar cracks with curved fronts, adopting either circular or elliptical shapes. These are problems that have been successfully modeled using standard finite element algorithms in the past. Normally, however, constructing finite element meshes that explicitly fit the crack front geometry is a labor-intensive process. This is true even though the crack surfaces are relatively simple to describe. Here, in general we employ finite element meshes that are very simple to construct in three dimensions, and which obviously are not fitted to the crack geometry. The point is to demonstrate that the method nevertheless provides reasonably accurate results.

3.1 Penny Crack

We consider a circular penny crack embedded in a domain subjected to far-field tension, in which case the loading is pure Mode-I. The results were obtained using a structured Cartesian mesh on a cube with side length of 4 units, with 200 nodes on each side. The Young's modulus of the material is 207,000 and Poisson's ratio is 0.3. The radius of the crack was taken to be of length $r = 1.0$. A constant normal traction of 100 is applied to the top surface. This problem and the other problems shown here are verifications against analytical solutions, so no unit system is implied and all results are dimensionless.

We compare results to the analytical solution to this problem for a penny-shaped crack in an infinite domain. To account for the finite size of the actual computational domain used, a scaling factor of 2.213 is applied, as described in [5]. The results are shown in Figure 5. We note that the X-FEM approximation consistently under-predicts the analytical result, even though these results correspond to a very refined mesh for this problem. This discrepancy may be due to the artificial crack front geometry that results from using only Heaviside enrichment, as discussed in the Introduction and Section 2.

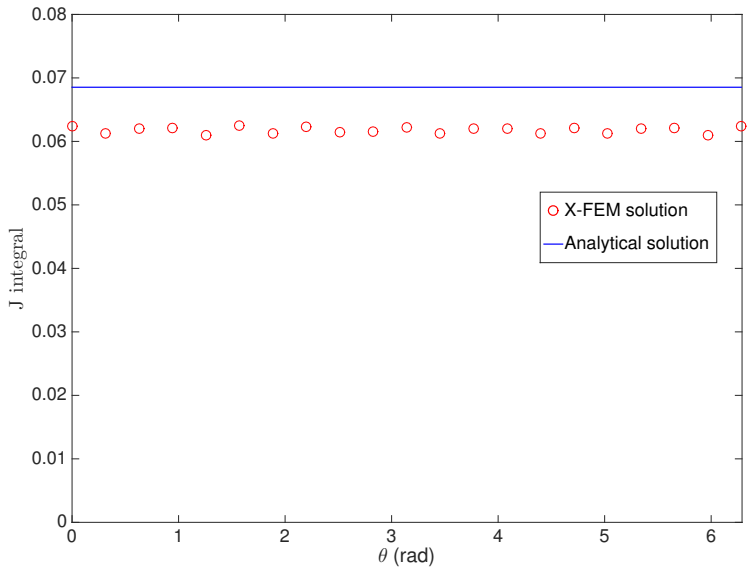

Figure 5: Variation of J-Integral (in dimensionless units) along the crack front for a flat, penny-shaped crack subjected to pure Mode-I loading. Results were obtained using a structured Cartesian mesh.

We further study this issue by building a finite element mesh that is curved to match the geometry of the crack front. While this approach is impractical for most cases, for simple cases such as this it is possible. Further, it minimizes the role of the artificial crack geometry. The mesh used for this problem and its deformation with a penny-shaped crack represented with the X-FEM under Mode-I loading are shown in Figure 6. The results are shown for a penny-shaped crack with radius $r = 0.2$ in Figure 7. A scaling factor was not used in this case as the size of the crack is relatively small compared to the computational domain. Compared to the results shown in Figure 5, we see a slight improvement in the accuracy of the results. However, there is also a small oscillation in the results, which may be due to a small mismatch between the mesh and the domains used for the J-integral.

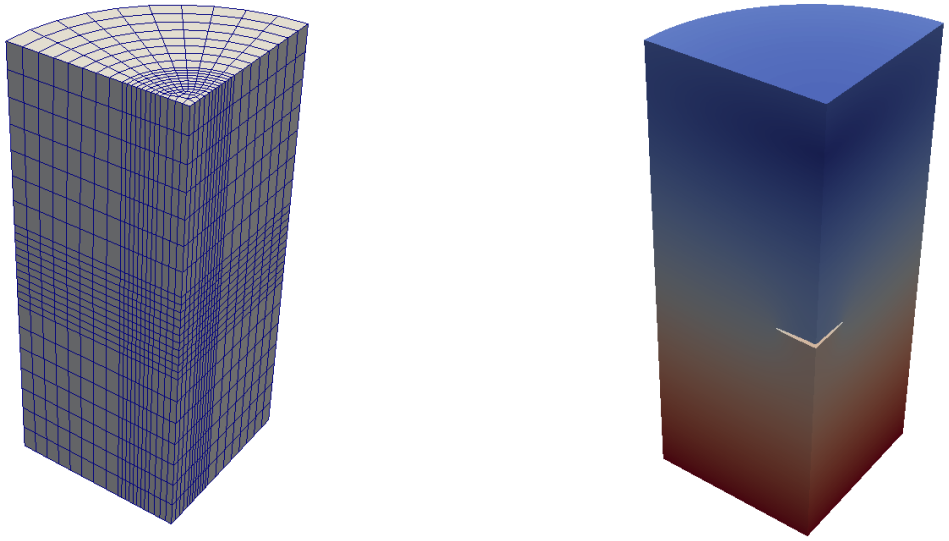

(a) (b)

Figure 6: (a) X-FEM mesh for a penny-shaped crack. (b) The displacement under Mode-I loading (scaled by a factor of 10).

3.2 Inclined Elliptical Crack

We now consider an inclined elliptical crack centrally located in a cube that is subjected to uniform tension. The ellipse has a major axis of $a = 0.6$ and minor axis of $b = 0.3$, and is oriented at an angle of 45 degrees with respect to the applied load. The same material properties and loading for the penny crack are used here. Results were obtained using a mesh with 100 elements on each side of a cube of side lengths $4 \times 4 \times 4$. 20 points were placed uniformly around the perimeter of the ellipse to calculate the stress intensity factors. The results are shown in Figure 8, with a comparison to the solution given in [6].

These results are comparable to what was observed for the penny crack problem on a similar mesh. The numerical results roughly follow the analytical solution, with some minor oscillation. These results can be improved considerably with mesh refinement. Doubling the number of elements on each side of the cube results in SIFs shown in Figure 9. The level of accuracy is impressive given that near-tip enrichment was not included in the formulation. We note that to some extent, small oscillations in the stress-intensity factors

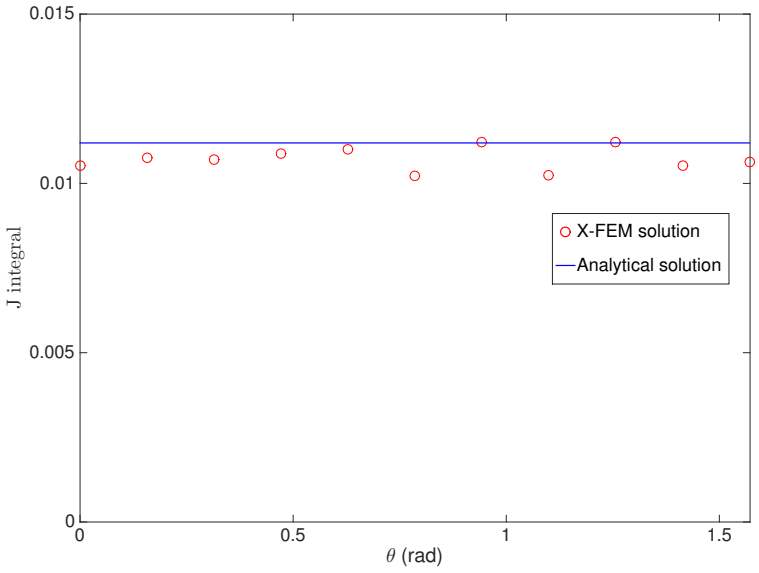

Figure 7: J-Integral in dimensionless units for a flat, penny-shaped crack subjected to pure Mode-I loading. Results were obtained using a mesh that is structured to conform to the crack geometry.

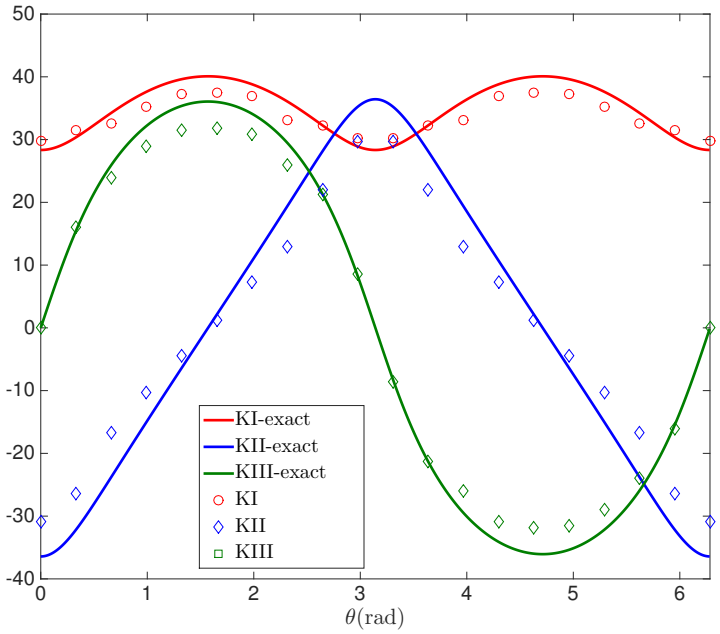

Figure 8: Stress intensity factors (dimensionless) for an inclined elliptical crack subjected to far-field loading, for a structured Cartesian mesh with 100 elements on each side.

are filtered out in the current approach through a judicious choice of sample point spacing along the crack front. If instead we choose 40 equally-spaced points around the perimeter of the ellipse, the results shown in Figure 10 are obtained. In this case, small oscillations in the crack-front SIFs can be observed once again.

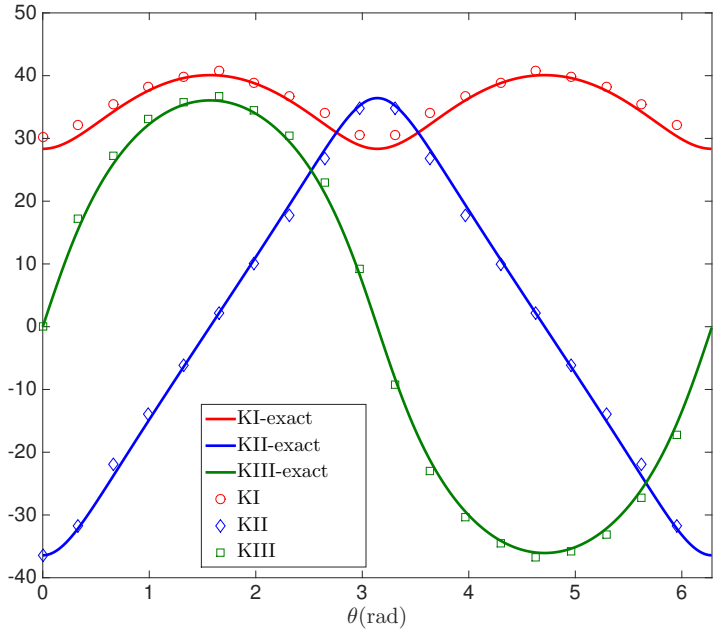

Figure 9: Stress intensity factors (dimensionless) for an inclined elliptical crack subjected to far-field loading, for a structured Cartesian mesh with 200 elements on each side. SIFs were obtained using 20 equally spaced points along the front.

One approach to effectively smoothing these small oscillations is to increase the width of the band for the scalar function q that is used in the interaction integral. Doubling the width of the domain used for the interaction integral yields the results shown in Figure 11.

These results indicate that even without near-tip enrichment, the X-FEM produces results that converge to known exact solutions for both mode-I and mixed mode loading scenarios. Using wider bands for the q function appears to be a reasonable and easily implemented technique for smoothing out the variation in the fracture integrals along the crack front.

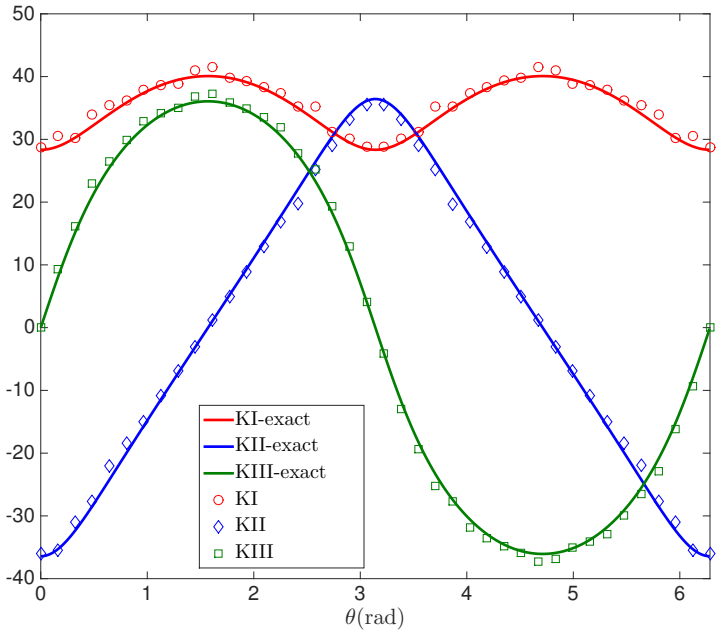

Figure 10: Stress intensity factors (dimensionless) for an inclined elliptical crack subjected to far-field loading, using 40 equally spaced points along the front.

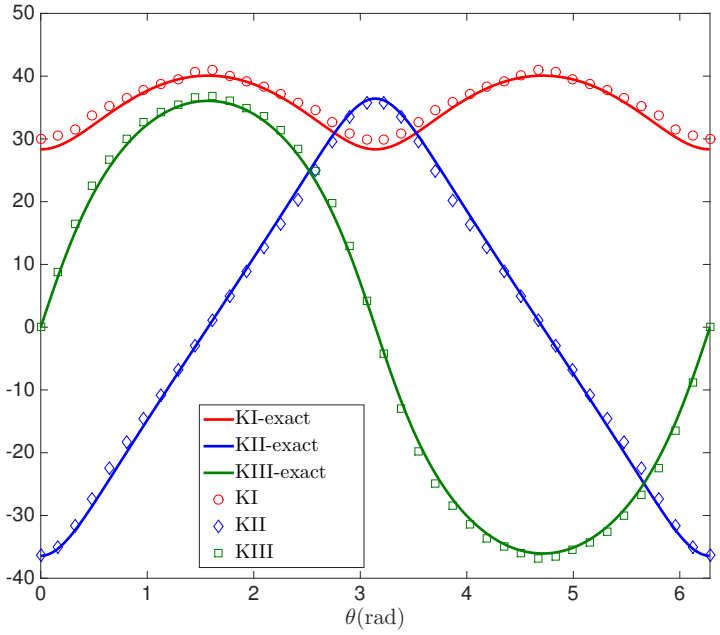

Figure 11: Stress intensity factors (dimensionless) for an inclined elliptical crack subjected to far-field loading, using 40 equally spaced points along the front and an increased width for the crack-tip weight function q.

4 Summary

Grizzly's capabilities were enhanced to allow for the calculation of SIFs for cracks that are arbitrarily placed with respect to a three-dimensional finite element mesh. The mesh cutting algorithm for three-dimensional problems was tested and modified to permit the definition of arbitrary elliptical cracks. In addition, modifications were made to the interaction integral routines to allow for SIFs to be extracted at arbitrarily specified points. Results of benchmark calculations indicate that reasonably accurate stress intensity factors can be calculated using these techniques, provided that sufficiently fine meshes are used.

The results of our benchmark calculations clearly indicate that the X-FEM methodologies work reasonably well, even without near-tip enrichment. However, in practice the need for very refined meshes can be somewhat limiting. In practical applications, models can easily be quite large, and it may not be feasible to have a very refined mesh throughout the domain. One area for future work is clearly to incorporate the asymptotic near-tip enrichment functions that are used in the standard X-FEM. These functions are well known to yield significant improvements in accuracy, even on relatively coarse meshes.

The X-FEM is expected be able to facilitate solution of some fairly challenging fracture mechanics problems related to surface-breaking flaws in reactor pressure vessels (RPVs) that extend through the stainless steel liner and slightly into the base metal. These flaws are a particular concern because of the thermally-induced stresses in the vicinity of that interface because of the mismatch in the coefficient of thermal expansion for the two materials. Incorporating those flaws in a mesh fitted to the flaw geometry can be extremely challenging, but the X-FEM can greatly facilitate the solution of that problem. With either a fitted mesh or the X-FEM, special care would need to be taken to properly identify and use the appropriate near-tip enrichment functions, and also modify the interaction integral routines to account for discontinuities in the material properties to solve this problem.

In addition to the application of the X-FEM to LEFM analysis of stationary cracks shown here, there are multiple other uses for the X-FEM in Grizzly that would facilitate the solution of problems of interest for age-related degradation in nuclear power plant components. Cohesive zone models for fracture of RPV steel have been developed previously, and with additional development, these can be incorporated into Grizzly using the X-FEM to permit mesh-independent propagation of cohesive fracture. There is also work underway to develop crystal plasticity models in Grizzly for irradiated RPV steel at the grain scale. The X-FEM implementation in Grizzly can be modified to permit its use for modeling boundaries between neighboring grains. The X-FEM can also be applied to model discrete fracture of concrete subjected to aging mechanisms in conjunction with models already under development.

5 References

1. C.L. Richardson, J. Hegemann, E. Sifakis, J. Hellrung, and J. M. Teran. An xfem method for modeling geometrically elaborate crack propagation in brittle materials. *International Journal for Numerical Methods in Engineering*, 88(10):1042–1065, 2011.

2. N. Moës, J. Dolbow, and T. Belytschko. A finite element method for crack growth without remeshing. *International Journal for Numerical Methods in Engineering*, 46(1):131–150, 1999.

3. A. Hansbo and P. Hansbo. A finite element method for the simulation of strong and weak discontinuities in solid mechanics. *Computer Methods in Applied Mechanics and Engineering*, 193(33-35):3523–3540, 2004.

4. P.M.A. Areias and T. Belytschko. A comment on the article "A finite element method for simulation of strong and weak discontinuities in solid mechanics" by A. Hansbo and P. Hansbo Comput. Methods Appl. Mech. Engrg. 193 (2004) 3523-3540. *Computer Methods in Applied Mechanics and Engineering*, 195(9-12):1275–1276, 2006.

5. S. Li, M.E. Mear, and L. Xiao. Symmetric weak-form integral equation method for three-dimensional fracture analysis. *Computer Methods in Applied Mechanics and Engineering*, 151(3-4):435–459, January 1998.

6. Hiroshi Tada, Paul C. Paris, and George R. Irwin. *The Stress Analysis of Cracks Handbook, Third Edition*. ASME, Three Park Avenue New York, NY 10016-5990, January 2000.